MOVING FROM TEMPORAL COHERENCE TO DECORRELATION TIME OF INTERFEROMETRIC MEASUREMENTS EXPLOITING ESA'S SAR ARCHIVE

Michael Foumelis [(1)], Zina Mitraka [(2)], Roberto Cuccu [(3,4)], Yves-Louis Desnos [(5)], Marcus Engdahl [(5)]

[(1)] RSAC c/o ESA-ESRIN, Science, Applications and Future Technologies Department, Via Galileo Galilei, 00044 Frascati, Italy, Email: michael.foumelis@esa.int
[(2)] Foundation for Research and Technology – Hellas (FORTH), N. Plastira 100, Vassilika Vouton, 70013 Heraklion, Greece, Email: mitraka@iacm.forth.gr

[(3)] ESA Research and Service Support, Via Galileo Galilei, 00044 Frascati, Italy, Email: roberto.cuccu@esa.int

[(4)] Progressive Systems Srl, Parco Scientifico di Tor Vergata, 00133 Roma, Italy.

[(5)] ESA-ESRIN, Science, Applications and Future Technologies Department, Via Galileo Galilei, 00044 Frascati, Italy, Emails: yves-louis.desnsos@esa.int, marcus.engdahl@esa.int

ABSTRACT

Interferometric coherence can be considered as an expression of temporal decorrelation. It is understood that interferometric coherence decreases with time between SAR acquisitions because of changes in surface reflectivity, reducing the quality of SAR phase measurements. This is an intrinsic characteristic of the design of SAR systems that has a significant contribution at longer time scales. Although in the past there was not sufficient amount of SAR data to extract robust statistical metrics for decorrelation, in the present study it is demonstrated that tailored analysis of interferometric coherence exploiting the large SAR archive available by the European Space Agency (ESA), enables the accurate quantification of temporal decorrelation. A methodology to translate the observed rate of coherence loss into decorrelation times over a volcanic landscape, namely the Santorini volcanic complex is the subject treated in this study. Specifically, a sensitivity analysis was performed on a large data stack of interferometric pairs to quantify at a pixel level the time beyond which the interferometric phase becomes practically unusable due to the effect of decorrelation. Though the dependence of decorrelation on various land cover/use types is already documented the provision of additional information regarding the expected time of decorrelation is of practical use especially when EO data are utilized in operational activities. The performed analysis is viewed within the improved capacity of current and future SAR systems, while underlining the necessity for exploitation of archive data.

1. INTRODUCTION

Following a plethora of validations and demonstrations, SAR Interferometry (InSAR) has been established as a mature space geodetic technique. One of the main advantages of space borne SAR systems with respect to GNSS is the continuous spatial coverage. However, the impact of temporal decorrelation especially in repeat-pass interferometry has been observed during the historical development of InSAR applications. It is understood that interferometric coherence decreases with time between SAR acquisitions because of changes in surface reflectivity, reducing the quality of SAR phase measurements. However, this is exactly the reason why coherence contains intrinsic information about the land surface characteristics.

Multiple studies have shown the applicability of InSAR coherence for various applications including land cover classification [1,2], monitoring forests and estimation of biophysical properties [3,4], glacier motion [5] as well as damage mapping [6]. The use of single coherence products as well as multi-temporal ones within operational frameworks is elaborated in [7].

Often, the multi-temporal dimension given in studies dealing with coherence change detection is limited to a small number of well-selected SAR acquisitions suited temporally to the application in hand. The emergence of SAR systems able to provide systematic acquisitions, such as the Sentinel-1 mission, is expected to introduce major change in the concept of monitoring InSAR coherence. Apart from foreseen advancement in coherence analysis, the availability of significant number of archived data from previous SAR missions of the European Space Agency (ESA) consist a wealth of information that still to be exploited.

Thus, the objective of this study is to demonstrate a potential usage of ESA's SAR archives presenting an approach that builds on these large data stacks in a more systematic matter. The work mainly involve implementation of already known concepts for temporal coherence monitoring. Though, by introducing tailored post-processing of coherence observables in a multi-temporal analysis framework a novel product is presented expressing the overall behaviour of coherence in time.

In the following chapters the rationale behind the proposed technique is presented, then the adopted

Proc. 'Fringe 2015 Workshop', Frascati, Italy
23–27 March 2015 (ESA SP-731, May 2015)

processing scheme is described and results are shown over a selected pilot site. The discussion part is dedicated to the assessment of the robustness of the obtained products, the type of information retrieved and finally future ideas of how this technique might evolve.

2. RATIONALE

Interferometric coherence is a well-defined parameter used as an measure of the quality of the interferometric phase in InSAR-related applications [8,9]. However, the assumptions required to measure this quantity from InSAR data implies the use of coherence as an estimation rather that an actual direct measurement. In fact, most common practice for calculating InSAR coherence is the use of maximum likelihood estimator [10,11], underlining exactly the type of calculations performed. Though, many alternative approaches have been proposed to accurately estimate interferometric coherence from SAR data [12,13,14].

The various sources of decorrelation can be elaborated in the following formula shown in [10]:

$$\gamma_{total} = \gamma_{thermal} + \gamma_{geometrical} + \gamma_{temporal}$$

where $\gamma_{thermal}$, $\gamma_{geometrical}$ and $\gamma_{temporal}$ the thermal, geometrical and temporal decorrelation terms, respectively

Changes caused by the different viewing angles of SAR antennas in repeat-pass configuration (geometric baseline), pixel mis-registration and the rotation of the targets with respect to the radar line-of-sight, all sum up to the geometrical decorrelation term. This term can be partly compensated for by selecting InSAR pairs of shorter the perpendicular baselines. Coherence loss due to thermal noise could be considered negligible compared to the other decorrelation sources. It is expressed by the signal to noise ratio of the InSAR measurements. Thus, interferometric coherence can be considered, under the above mentioned assumptions, as an expression of temporal decorrelation.

Investigation of coherence behaviour in time and hence, indirectly of temporal decorrelation, was also the subject of previous studies [15]. The idea was basically related to predicting the approximate quality of an interferogram using simple inputs as the values of temporal and geometric baselines.

In our case, a stack of InSAR coherence levels is utilized in order to directly quantify the temporal decorrelation term for the specific area of interest. The general concept is to generate a product providing information of the time required for the InSAR phase to decorrelate, that is when coherence decreases beyond a selected threshold.

This is achieved by fitting a model describing the decay of coherence in time to the original InSAR inputs. Since this procedure is applied on a pixel basis, which results in increased computational demands a sea mask is introduced (extracted from any external elevation source), to restrict the analysis over land. Visual inspection of the obtained model fit can be evaluated in coherence versus day difference plots. The output showing Decorrelation Time (DT) estimate is finally obtained by selecting a coherence threshold and finding the corresponding days difference (dt value) at the intersection with the fitted model. Different DT maps for corresponding coherence thresholds can then be calculated subject to the requirements of the specific application.

Apart from the decorrelation times, by-products of the coherence modelling are the estimated models' coefficients as well as the obtained fit as described by R^2. Since the analysis is performed on a pixel basis the additional parameters were estimated through the modelling comprise and additional source of information.

3. PILOT SITE SELECTION AND DATA USED

The pilot site selected for the demonstration of the proposed technique is the Santorini Volcanic Complex located in the southern part of the Aegean Sea (Greece) (Fig. 1). The geological setting of Santorini as well as complex relief offers a unique setting for such analysis. In addition, the deformation field of the volcano, as derived from InSAR [16,17] and other geodetic techniques [18,19,20,21], indicate the lack of significant displacements in the period 1992-2010 that would potentially contribute to decorrelation over large temporal spans. Furthermore, the availability of geodetic networks (GPS and levelling) in the island for monitoring its volcanic activity highlight the necessity for evaluation of the capacity of repeat-pass SAR interferometry for deformation mapping in a more quantitative manner.

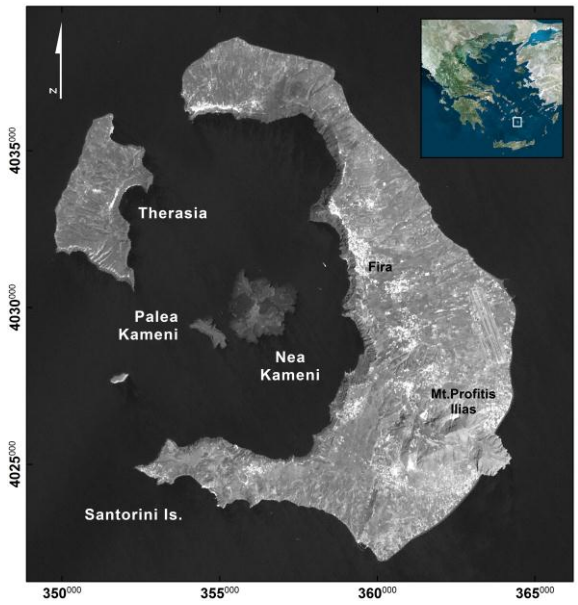

Figure 1. Location map of the study area.

For the purposes of the study the entire ESA SAR archive of ERS-1/-2 and ENVISAT over the selected pilot site was used, consisting of 30 and 66 scenes for the ascending track 329 and the descending track 150, respectively. These SAR data stacks cover a period of approximately 18 years which is sufficient to derive robust estimates for temporal decorrelation.

4. PROCESSING ON ESA'S G-POD

Processing of SAR data was performed using the GAMMA software packages [22], following commonly applied chains in deformation related studies [23,24].
An important aspect of the processing was the estimation of the coherence using an adaptive procedure as described in [25]. This ensures unbiased estimations, retaining high coherence levels over build-up areas and rock outcrops, and lower values for fast decorrelating regions such as water bodies and agricultural fields. Estimations were applied over several resolution elements, complex multi-looking (by factors 1x5 in range and azimuth, respectively) to reduce speckle in the interferograms. The average coherence levels calculated as the mean of the corresponding coherence stack for both acquisition geometries are shown in Fig. (2).
The entire processing was performed on ESA's Grid Processing on Demand (G-POD) facilities, a Grid and Cloud-based operational environment, where Earth Observation (EO) scientific algorithms can be integrated as services to exploit the available EO data collections from the interconnected archives. The G-POD system offers a winning combination of both high performance computing and fast data access by adopting the concept to bring the processor close to the data and run parallel instances on the several available worker nodes. The scientific user takes advantage of this solution by saving a considerable amount of time, computing resources and storage facilities with respect to the processing carried out on a local workstation. The application workflow exploited on the G-POD environment for the present work is based on two main modules. The first module performs the SAR data co-registration, the definition of the interferometric pairs, the coherence stack estimation and geocoding. The second module takes in input the previous generated coherence stack, applies the model fitting algorithm and produces the final outputs (Fig. 3).
As already mentioned, the necessity to reduce the geometrical decorrelation effects on coherence, dictate the constraint of the perpendicular baselines (Bp) of the InSAR stack. In our case, an upper bound was considered taking into account interferometric pairs with $Bp \leq 100$m. Based on the above mentioned constraints a total number of 22 interferometric pairs for the ascending and 99 pairs for the descending track were formed and coherence levels were estimated. Even though no cross-InSAR between ERS-ENVISAT data was realised, coherences from both missions were commonly analysed in the subsequent post-processing steps, increasing substantially the number of input observations per acquisition geometry. It should be noted that layover and shadow regions for the corresponding acquisition geometries were masked out and no further calculations were performed.

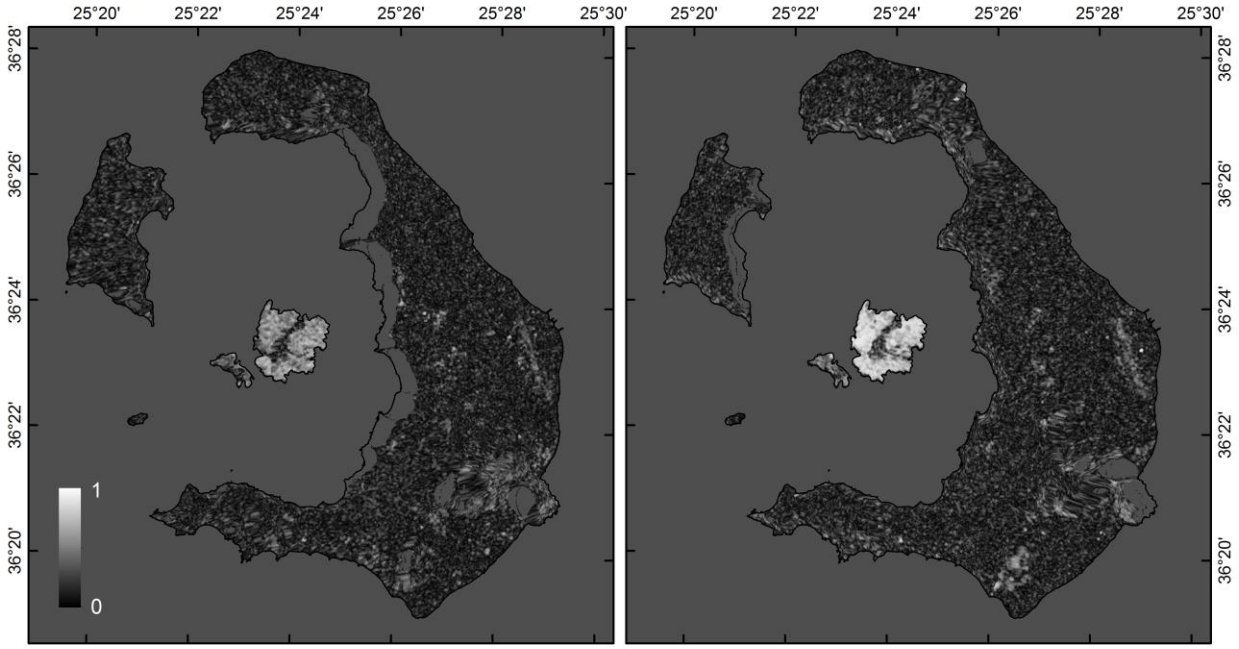

Figure 2. Average coherence levels in ascending (left) and descending (right) acquisition geometry. Layover and shadow regions are masked.

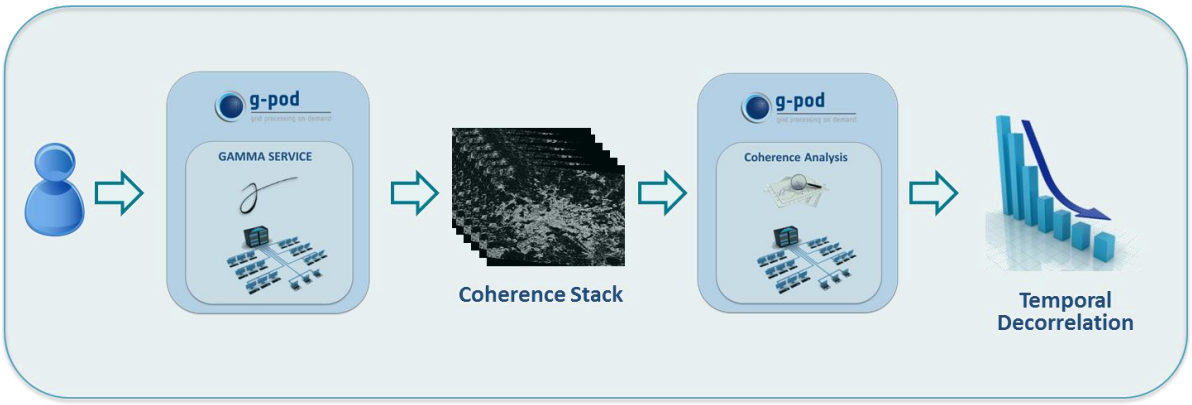

Figure 3. Processing scheme implemented on ESA's G-POD for the analysis of the SAR data.

Having seamlessly overlapping geocoded coherence stacks, further processing was possible. The following steps included fitting using models based on literature review for coherence temporal loss (Fig. 4). The models applied consider an exponential decay of coherence with time, enforcing in both cases the starting point to x=0 & y=1, assuming that InSAR pairs with zero temporal span should exhibit at least theoretically maximum coherence levels. Two single-parameter models were fitted based on literature review ($\exp(-a\cdot x)$ & $\exp(-a\cdot x^2)$), while a two-parameters model ($\exp(-a\cdot x+b)$ was also applied airing form the behaviour of the data themselves. The residuals for each model as well as the goodness of fit as described by the R^2 coefficient were considered to evaluate quantitatively the obtained results.

In Figure 5 the obtained results for both ascending and descending tracks using a coherence threshold of 0.3, commonly defined as the minimum value for accepting InSAR phase information, are shown.

5. DECORRELATION TIME ESTIMATES

Post-processing of coherence images by means of multi-temporal analysis provided per pixel estimates of decorrelation time over the area of interest.

Higher decorrelation times were observed at the bare volcanic rocks outcropping at Palaia and Nea Kameni islands exceeded 3200 days. Local patterns are recognised over urban areas within the dominant low coherence and shorter decorrelation times at the surrounding regions. Moderate DT values are calculated for the basement Alpine rocks at Mt. Profitis Ilias at the southeastern mountainous part of Santorini (Fig. 5).

The results are in agreement with the calculated average temporal coherence levels (Fig. 2). However, it is interesting to observe that the decorrelation time estimates do not suffer from spatial variability over low coherence regions. Exploiting large number of coherence observations allows for a smoother presentation of neighbouring pixels belonging to a common land surface type.

Changes in the thresholds for calculating the DT map (Fig. 6) directly reflect the characteristics of the land surface. An example is shown for the Palaia and Nea Kameni islands were the changes correspond to the different lava types and possibly their weathering conditions. For higher thresholds lower DT values are typically obtained, whereas when decreasing coherence thresholds more details are recognised in the DT maps since the range of values is quite larger.

An important fact is the fitting over regions of extremely high coherence. In these cases, the fitted models were always being higher than the lowest selected coherence threshold (=0.3), indicating that decorrelation is not reached over the examined temporal span. For these pixels the largest day differences of the input InSAR pairs were assigned to. It can be seen that this is causing a saturation of the decorrelation time estimate for low coherence thresholds (Fig. 6).

In terms of robustness the results of coherence modelling indicates generally moderate fits (on average R^2=0.45), a fact which indicate the residual effects from geometric decorrelation terms. It is of interest that coherence remains quite higher than what predicted by the various models for long time intervals. This could be attributed to the contamination of the coherence estimate from the presence of dominant point-like scatterers within the resolution cells.

6. DISCUSSION

It was shown that by combining through temporal analysis an interferometric coherence stack an estimate of the decorrelation times at a pixel level could be obtained. The advantage of the proposed technique is that a single product is generated describing the temporal behaviour of coherence for each resolution cell. In addition, having decorrelation directly expressed in units of time (e.g. days) allows relatively easier interpretation and further usability compared to the values of the coherence estimates.

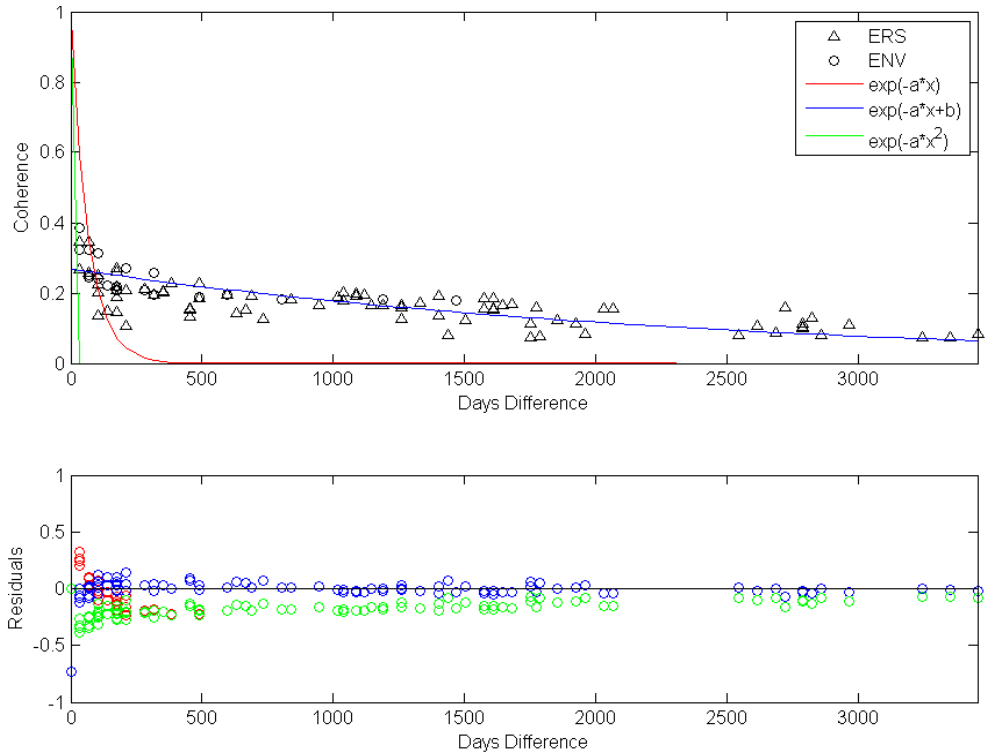

Figure 4. Diagram showing the behaviour of the average coherence over time for the descending geometry (up). Different models are fitted to describe the coherence loss in time. Models' residuals are also shown (down).

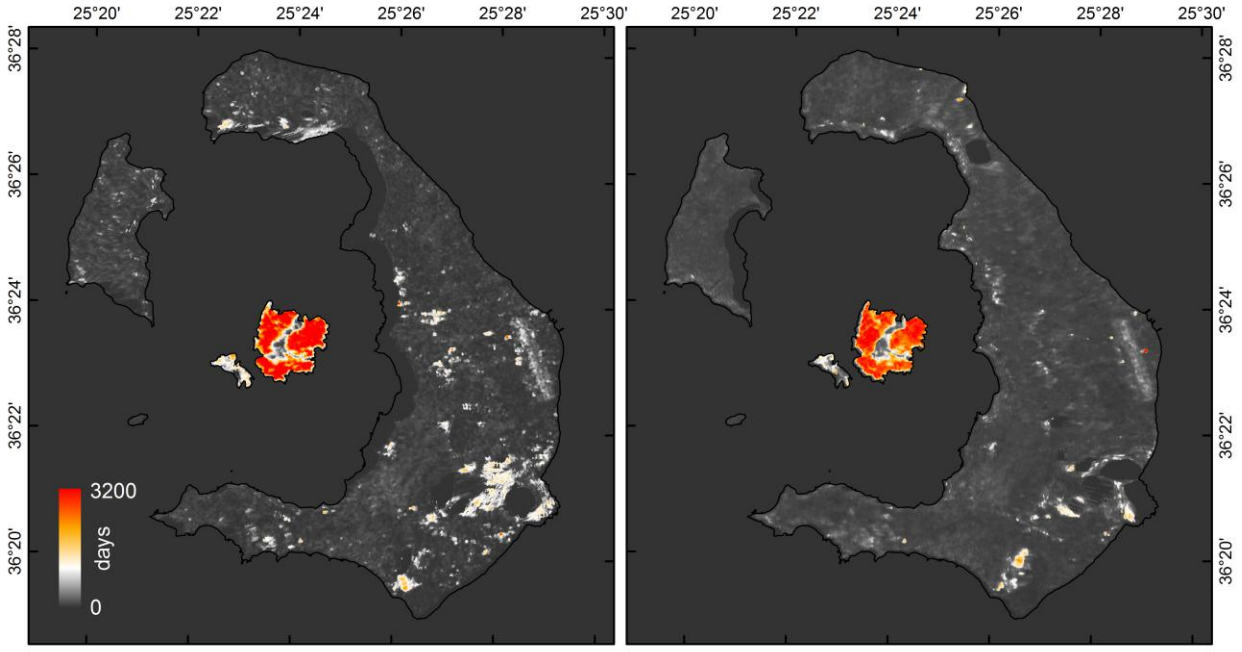

Figure 5. Decorrelation times for the area of interest as estimated by the proposed multi-temporal analysis technique for a coherence threshold of 0.4.

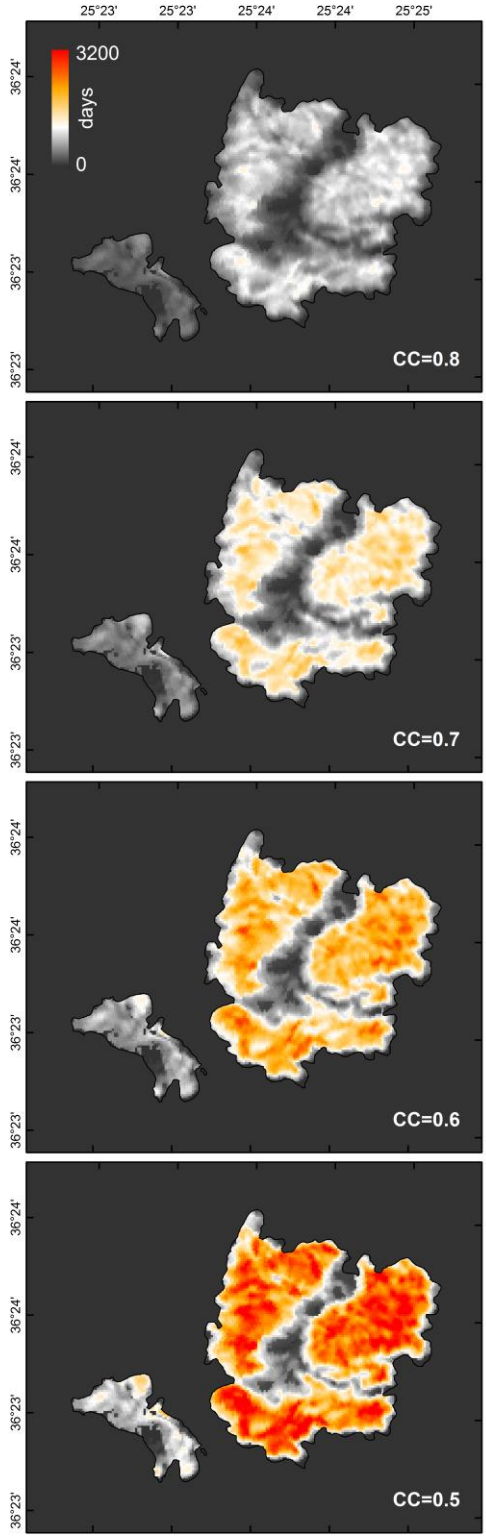

Figure 6. Decorrelation times over the Palea and Nea Kameni Is. for different coherence thresholds. Shorter decorrelation times are obtained for higher coherence thresholds.

Constraining the inputs considering only interferometric pairs of short perpendicular baselines is of importance to minimise the effect of the geometric decorrelation. However, an overall assumption on the negligible contribution of other sources of decorrelation is still required. Then, the estimated decorrelation times might be fully attributed to the temporal decorrelation term. This information could be then directly linked to the characteristics of the land surface, aiding land cover/use classification, especially for mapping urban areas.

Since the majority of geohazards rely on long term observation scenarios, the effect of temporal decorrelation is evident as coherence becomes dominated by temporal changes. The estimation and mapping within a geostatistical context of the spatial distribution of the temporal decorrelation times in an area without a necessary a priori knowledge of its surface characteristics is a fundamental parameter for the design and establishment of local GNSS networks as well as the definition of optimal monitoring strategy for various geohazards.

The "as expected" outcome of the decorrelation time analysis provide a solid ground for its implementation and further performance testing over other environments. Potential limitation of the applicability of the proposed technique might be for regions of significant temporal changes (e.g. agricultural fields). Such regions present high coherence variability as being effected by non-physical processes, random human-induced surface changes, adding more outliers and effecting the modelling of decorrelation.

Furthermore, the dependency of the modelling on long time interval coherence estimates is still to be further investigated. This becomes more critical when dealing with low coherence levels. It should be noted though that higher coherence values are estimated for such long temporal span InSAR pairs compared to the overall fitted models. Finally, it seems that the robustness of the results is highly depended on the number and the temporal distribution of the inputs, a requirement that underline the necessity for systematic SAR observations.

The processing for this work was performed exploiting the ESA's G-POD infrastructure by running the software modules instances in a less automated way in order also to verify and test the feasibility of the their integration and chaining as operating service. Future implementation of the proposed analysis as a service for scientists is foreseen, providing an easy and configurable way to obtained results starting from ingestion of SAR data, interferometric processing for coherence estimation to decorrelation time analysis.

Taking into account the promising results already presented using Senitnel-1A coherence [26], the above mentioned activity seems even more valuable considering the large amount of data collected by the Sentinel-1 mission, both in terms of volume and file sizes, and the requisite for their systematic processing.

7. ACKNOWLEDGES

ERS and ENVISAT SAR data were provided by ESA under Cat-1 project 3333.

8. REFERENCES

1. Bruzzone, L., Marconcini, M., Wegmüller, U. & Wiesmann, A. (2004). An Advanced System for the Automatic Classification of Multitemporal SAR Images. *IEEE Transactions on Geosciences and Remote Sensing*, 42(6), 1321-1334.

2. Wegmüller, U., Strozzi, T., Farr, T. & Werner, C.L. (2000). Arid Land Surface Characterization with Repeat-Pass SAR Interferometry. *IEEE Transactions on Geosciences and Remote Sensing*, 38(2), 776-781.

3. Santoro, M., Askne, J.I.H., Wegmüller, U. & Werner, C.L. (2007). Observations, Modeling, and Applications of ERS-ENVISAT Coherence Over Land Surfaces. *IEEE Transactions on Geosciences and Remote Sensing*, 45(8), 2600-2611.

4. Koskinen, J.T., Pulliainen, J.T., Hyyppä, J.M., Engdahl, M.E. & Hallikainen, M.T. (2011). The Seasonal Behavior of Interferometric Coherence in Boreal Forest. *IEEE Transactions on Geosciences and Remote Sensing*, 39(4), 820-829.

5. Strozzi, T., Luckman, A., Murray, T., Wegmuller, U. & Werner, C.L. (2003). Glacier motion estimation using SAR offset-tracking procedures. *IEEE Transactions on Geoscience and Remote Sensing*, 40(11), 2384-2391.

6. Hoffmann, J. (2007). Mapping damage during the Bam (Iran) earthquake using interferometric coherence, *International Journal of Remote Sensing*, 28(6), 1199-1216.

7. Yun, S-H., Milillo, P., Simons, M., Owen, S., Webb, F., Fielding, E.J., Hua, H., Milillo, G., Coletta, A., Rosen, P. & Dini, L. (2015). Interferometric Coherence for Rapid Disaster Response. Proc. of FRINGE, ESA SP-731 (CD-ROM), ESA Publications Division, European Space Agency, Noordwijk, The Netherlands.

8. Just, D. & Bamler, R. (1994). Phase statistics of interferograms with applications to synthetic aperture radar. *Journal of Applied Optics*, 33(20), 4361-4368.

9. Hanssen, R.F. (2001). Radar Interferometry: Data interpretation and error analysis. Kluwer Academic Press, Dordrecht, The Netherlands, 298p.

10. Zebker, H.A. & Villasenor, J. (1992). Decorrelation in interferometric radar echoes. *IEEE Transactions on Geoscience and Remote Sensing*, 30(5), 950-959.

11. Seymour, M.S. & Cumming, I.G. (1944). Maximum Likelihood Estimation For SAR Interferometry. Proc. of IGARSS, Pasadena, CA, USA, 8-12 August, vol. 4, pp. 2272-2275.

12. Cattabeni, M., Monti-Guarnieri, A. & Rocca, F. (1994). Estimation and Improvement of Coherence in SAR Interferograms. Proc. of IGARSS, Pasadena, CA, USA, 8-12 August, vol. 2, pp. 720-722.

13. Zebker, H.A. & Chen, K. (2005). Accurate Estimation of Correlation in InSAR Observations. *IEEE Geosciences and Remote Sensing Letters*, 2(2), 124-127.

14. Jiang, M., Ding, X. & Li Z. (2014). Hybrid Approach for Unbiased Coherence Estimation for Multitemporal InSAR. *IEEE Transactions on Geosciences and Remote Sensing*, 52(5), 2459-2473.

15. Chaabane, F., Tupin, F. & Maître, H. (2005). An empirical model for interferometric coherence. Proc. of SPIE 'SAR Image Analysis, Modeling, and Techniques VII' (Ed. F. Posa), vol. 5980, pp. 132-140.

16. Papageorgiou, E., Foumelis, M. & Parcharidis, I. (2011a). SAR interferometric analysis of ground deformation at Santorini Volcano (Greece). Proc. of FRINGE, ESA SP-697 (CD-ROM), ESA Publications Division, European Space Agency, Noordwijk, The Netherlands.

17. Foumelis, M., Trasatti, E., Papageorgiou, E., Stramondo, S. & Parcharidis, I. 2013. Monitoring Santorini volcano (Greece) breathing from space. *Geophysical Journal International*, doi: 10.1093/gji/ggs135.

18. Papageorgiou, E., Tzanis, A., Sotiropoulos, P. & Lagios, E. (2010). DGPS and magnetotelluric constraints on the contemporary tectonics of the Santorini Volcanic Complex. Bulletin of the Geological Society of Greece, XLIII(1), 344-356.

19. Stiros, S.C., Psimoulis, P., Vougioukalakis, G. & Fyticas, M., 2010. Geodetic evidence and modeling of slow, small-scale inflation episode in the Thera (Santorini) volcano caldera, Aegean Sea, Tectonophysics, 494, 180– 190.

20. Papageorgiou, E. (2011b). Surface Deformation Study for the Volcanic Hazard Assessment Using Geophysical and Space Techniques: The Case of the Hellenic Volcanic Arc. Ph.D. dissertation, Dept. Geoph.-Geoth., Univ. of Athens, Athens, Greece, 397p, doi:10.12681/eadd/26334 (in Greek).

21. Lagios, E., Sakkas, V., Novali, F., Bellotti, F., Ferreti, A., Vlachou, K. & Dietrich, V. (2013).

SqueeSAR™ and GPS ground deformation monitoring of Santorini Volcano (1992-2012): Tectonic implications. Tectonophysics, http://dx.doi.org/ 10.1016/j.tecto.2013.03.012.

22. Wegmüller, U., Werner, C. & Strozzi, T. (1998). SAR interferometric and SAR differential interferometric processing chain. Proc. of IGARSS, Seattle, WA, USA, 6-10 July, vol. 2, pp. 1106-1108.

23. Papageorgiou, E., Foumelis, M. & Parcharidis, I. (2012). Long- and short-term deformation monitoring of Santorini Volcano: Unrest evidence by DInSAR analysis. *IEEE Journal of Selected Topics in Applied Earth Observations and Remote Sensing*, doi: 10.1109/JSTARS.2012.2198871.

24. Foumelis, M. (2012). Human induced groundwater level declination and physical rebound in northern Athens Basin (Greece) observed by multi-reference DInSAR techniques. Proc. of IGARSS, Munich, Germany, 22-27 July, 820-823.

25. Santoro, M., Werner, C. & Wegmüller, U. (2007). Improvement of interferometric SAR coherence estimates by slope-adaptive range common-band filtering. Proc. of IGARSS, Barcelona, Spain, 23-28 July, pp. 129-132.

26. Wegmüller, U., Santoro, M. & Werner, C. (2015). On the Estimation and Interpretation of Sentinel-1 TOPS InSAR Coherence. Proc. of FRINGE, ESA SP-731 (CD-ROM), ESA Publications Division, European Space Agency, Noordwijk, The Netherlands.